21Applied Sciences_Marwan2_rev1.docx

語数	7693	提出時間	2022-1月-29 11:03午前
		レポート ID	81948511

applied sciences

MDPI

Article

Detailed and Average Models of Grid Connected MMC Controlled Permanent Magnet Wind Turbine Generator

Marwan Rosyadi [1], *, Atsushi Umemura [2], Rion Takahashi [2] and Junji Tamura [2]

[1] Dept. of Electrical Engineering, Faculty of Engineering, Muhammadiyah University of Surabaya, Indonesia; rosyadi@um-surabaya.ac.id (M.R.)
[2] Dept. of Electrical and Electronic Engineering, Kitami Institute of Technology, Japan; umemura@mail.kitami-it.ac.jp (A.U.), rtaka@mail.kitami-it.ac.jp (R.T.), tamuraj@mail.kitami-it.ac.jp (J.T.)
* Correspondence: rosyadi@um-surabaya.ac.id (https://www.um-surabaya.ac.id)

Abstract: In this paper detailed model and average model of the MMC (Modular Multilevel Converter) controlled Permanent Magnet Synchronous Generator (PMSG) based direct drive wind turbine concept are proposed. The models are used to analyze the steady state and transient characteristics of the grid connectivity study of the wind turbine generator. Configuration of electrical topology and control scheme of the wind turbine generator for both models are comprehensively presented. In the detailed model, the MMC circuit is represented by power electronic IGBTs with switching phenomena considered. While in the average model, the MMC circuit is simplified by using voltage source representation, hence complexity of MMC circuit and simulation duration of the analysis can be reduced. Comparative analysis between the detailed and simplified models is also investigated through simulation performed by using PSCAD/EMTDC. The simulation results show that both models have a good controllability and dynamic stability in the cases of steady state and transient conditions. The simulation results also confirm that the average model has adequate accuracy and simulation time can be reduced significantly.

Keywords: Wind Turbine Generator; Modular Multilevel Converter; Permanent Magnet Synchronous Generator; Steady Stated and Transient Analyses; Grid connectivity study.

Citation: Last name, F.; Las tname, F.; Lastname, F. Title. *Appl. Sci.* **2021**, *11*, x. https://doi.org/10.3390/xxxxx

Academic Editor: First name Lastname

Received: date
Accepted: date
Published: date

1. Introduction

A few years earlier, Technologies of wind turbine generator have been increasing significantly in the size such as hub height, rotor diameter, and generator capacity to convert more power from wind energy with higher efficiency, lower investment and operating costs. In the early year of 2021, the power capacity of wind turbine generator has increased up to 15 MW [1], and in year of 2035 the capacity of wind turbine generator would be predicted to reach up to 17 MW [2]. Along with the increasing capacity, the connection of the wind turbine generators to grid power system by traditional two levels or three levels converters requires many powers electronic devices such as IGBTs in series or parallel connections to achieve very high power capacity and operating voltage. Modular Multilevel Converter (MMC) is a promising solution for high-power capacity wind power generation. Compared to other conventional converter technologies, the MMC is a novel converter concept that has many superiorities such as a simpler structure and flexible design which enables to expand the number of levels and replace the submodules easily, so that the maintenance handling becomes easy [3,4]. In addition, connecting the MMC to a grid system without a transformer is possible [5].

Implementation of MMC in wind power generator, however, has not been reported so much. Most of the reports are investigating about stability of grid connected wind farm connected via MMC based High Voltage Direct Current (HVDC) Transmission system [6-

10]. Only few papers discussed about topology concept of implementation of MMC controlled wind turbine generator. Investigation of performance and ~~opportunities~~ topology of MMC for 2 MW 0.69 kV and 10 MW 10 kV have been discussed in [11], however the study only discusses about the grid side converter and concenters at ~~opportunities topology for the MMC and~~ losses distribution between submodu[illegible] In [12], the application of MMC controlled multi-phase PMSG has been proposed. The fault tolerant control strategy of the MMC [illegible]alidated on simulation analysis with detailed model representation. It can be said that a comprehensive discussion about the modelling of MMC controlled wind turbine generat[illegible]for grid connectivity study has not been widely discussed.

Feasibility study on stability of wind turbine generator connecte[illegible]o grid system is particularly important in a wind farm design. The dynamic behavior under steady state and transient conditions of a wind farm will affect voltage and frequency stability of grid system. Large variation of energy production of a wind farm or out-of-synchronism of a huge capacity of wind farm due to a short circuit fault can have great impact on power system stability and power quality [13,14]. Therefore, modeling and simulation analyses of grid connectivity of wind farm in the early stage in development of wind farm is very essential.

In [illegible] paper, detailed and average models of grid connected MMC controlled Permanent Magnet Synchronous Generator (PMSG) based direct drive wind turbine are proposed. The models can be used as representation model of the wind turbine generator for grid connectivity study. PMSG was chosen on the basis that most manufacturers use this type of generator for their large-capacity wind turbine generators [15-17] due to its high efficiency and attractive features suitable for wind turbine concept.

In the detailed model, the MMC includes detailed representation of power electronic IGBT converters and the MMC circuit i[illegible]onfigured by sub-module which has two levels half bridge configuration composed of two IGBTs with anti-parallel diodes and a capacitor. As switching phenomenon with multi-carrier modulation technique is considered in the modeling, the model should be discretized at a relatively small simulation time step (10 microseconds). The detailed model is very suited for analyzing the dynamic performance of control systems and harmonics in a short duration ~~of the simulation~~.

In the average model, the MMC circuit with power electronic IGBT modules is represented by equivalent voltage sources generating ac voltages. Switching phenomenon is neglected, and hence this model allows using much larger simulation time step (100 microseconds). Therefore, the a[illegible]ge model is suited for simulation analysis of long time.

The organization of the paper can be summarized as follows: Section 2 presents the proposed detailed model of MMC controlled PMSG based wind turbine. Section 3 presents the proposed average model of MMC controlled PMSG based wind turbine. Section 4 discusses about simulation and analysis of grid connected ~~of a 50 MW~~ wind farm which consists of 5 (five) unit of 10 MW PMSG based wind turbine controlled by MMC system. The simulation and a[illegible]ysis focused on steady state and transient analyses of both proposed models which have been performed by using PSCAD/EMTDC. Finally, in Section 5 conclusions of the study are presented.

2. Detailed Model of MMC Controlled Wind Turbine Generator

Figure 1 show[illegible]onfiguration of MMC controlled wind turbine gener[illegible]r in the detailed model. The wind turbine generator is gearless system in which the wind turbine rotor directly drives rotor shaft of the PMSG. The PMSG is multipoles type of generator that operates at variable voltage and frequency. Electrical power produced b[illegible] the generator is supplied to grid system with constant voltage and frequency through back-to-back converter. The back-to-back converte[illegible]is formed from two MMCs, namely Stator side MMC and Grid side MMC which are linked by DC link circuit. Three phase ac voltage of PMSG stator winding is rectified by Stator Side MM[illegible], and the dc voltage of DC link circuit is inverted to AC voltage by Grid Side MMC. The Stator side MMC is connected to stator winding terminal of PMSG, and the Grid side MMC is connected to grid system through

a step-up transformer (TR). On the stator side MMC, $I_S^{(abc)}$ and $V_S^{(abc)}$ are respectively three phase currents and voltages from the stator winding, and ω_r is rotational speed of rotor shaft of the PMSG. On the grid side MMC, $I_G^{(abc)}$ and $V_G^{(abc)}$ are respectively three phase currents and voltages from the terminal of the grid side MMC. Each of the MMC system is equipped with the main MMC controller, inner MMC controller, and the Phase-Shifted Pulse Width Modulation (PS-PWM) circuit. The DC link circuit is configured by two capacitors (C_{dc}) arranged in series. The DC link circuit is also equipped with over voltage protection system controlled by a DC chopper. For more details, each part of detailed model of MMC controlled wind turbine generator would be explained as follows.

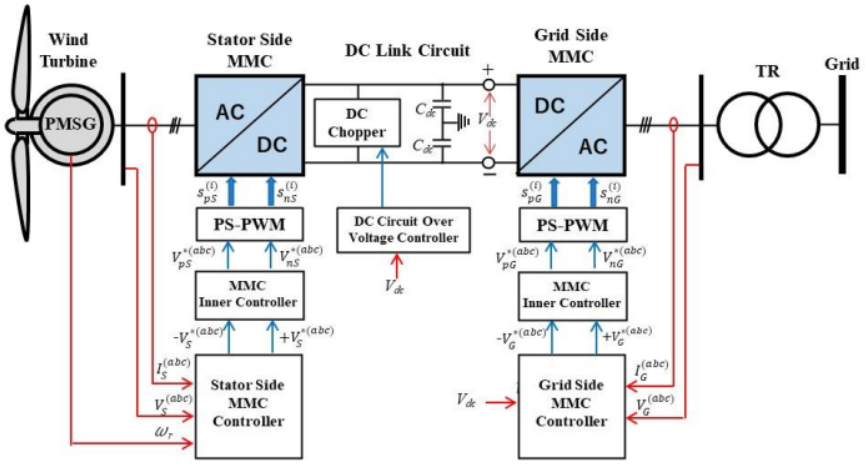

Figure 1. Configuration of MMC controlled wind turbine generator in detailed model.

2.1. Wind Turbine Model

2.1.1. Power conversion and characteristics of wind turbine

In this paper wind turbine direct driven generator with variable speed concept is considered. The actual mechanical power output of wind turbine extracted from wind can be written as follows [18]:

$$P_w = 0.5\ \rho\pi R^2\ V_w^3\ C_p(\lambda,\beta) \quad (1)$$

where, P_w is converted power from wind energy (W), R is rotor blade radius (m), V_w is wind velocity (m/s), ρ is air density (Kg/m³), and C_p is power coefficient. The C_p depends on characteristic wind turbine coefficients (c_1 to c_6), pitch angle (β) and tip speed ratio (λ) which can be calculated by the equations as follows [16]:

$$C_p(\lambda,\beta) = c_1\left(\frac{c_2}{\lambda_i}\ - c_3\ \beta - c_4\right)e^{\frac{-c_5}{\lambda_i}} + c_6\lambda \quad (2)$$

$$\frac{1}{\lambda_i} = \frac{1}{\lambda - 0.08\ \beta} - \frac{0.035}{\beta^3 + 1} \quad (3)$$

$$\lambda = \frac{\omega_r R}{V_w} \quad (4)$$

The values of characteristic coefficients of the wind turbine, c_1 to c_6, are 0.5176, 116, 0.4, 5, 21 and 0.0068, respectively [18], and ω_r is rotor speed of the wind turbine (rad/s).

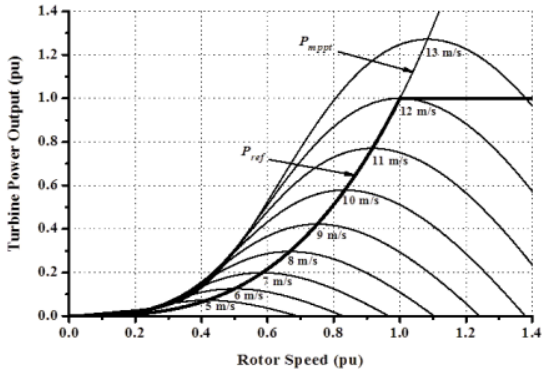

Figure 2. Turbine power output vs rotor speed characteristic

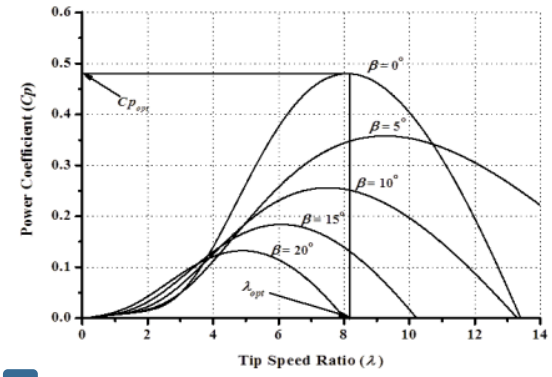

Figure 3. Power coefficient vs tip speed ratio characteristic of wind turbine

From Equations 1 to 4 the characteristics of wind turbine are shown in Figures 2 and 3. The relation of power output and rotor speed is depicted in Figure 2, and the relation of power coefficient and tip speed ratio characteristic is depicted in Figure 3. The optimum tip speed ratio (λ_{opt}) of 8.1 and the optimum power coefficient (Cp_{opt}) of 0.48 are obtained when wind velocity is at rated speed of 12 m/s. The wind turbine power output through Maximum Power Point Tracking (MPPT) is calculated as follows [19]:

$$P_{mppt} = 0.5\rho\ \pi\ R^2 \left(\frac{\omega_r R}{\lambda_{opt}}\right)^3 C_{popt} \quad (5)$$

while, the wind turbine reference power (P_{ref}) is limited to rated power 1.0 pu when the rotor speed is equivalent to or over rated speed 1.0 pu.

2.1.2. Drive train model

The moving parts of direct driven wind turbine generator are comprised of following components: rotor blades with pitching mechanism system, a hub, and rotor shaft. Generally, in the study of grid connectivity of wind turbine generator the drive train model is treated as two-lumped mass or one-lumped mass models [20]. Because the wind turbine generator in this study is totally seperated from the grid system by a back-to-back MMC system, hence, the one-lumped mass model of the drive train is considered here.

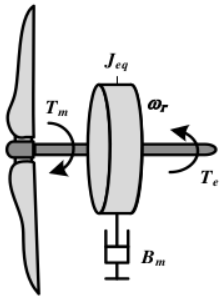

Figure 4. One-lumped mass model of wind turbine generator

The scheme of the drive train model in one-lumped mass model is given in Figure 4 which is represented by the following equation [20]:

$$\frac{d\omega_r}{dt} = \frac{T_e - T_m}{J_{eq}} - \frac{B_m}{J_{eq}}\omega_r \quad (6)$$

where T_m is the wind turbine mechanical torque (Nm), T_e is the generator electrical torque (Nm), J_{eq} is the equivalent rotational inertia of the wind turbine generator (kg.m²), and B_m is the damping coefficient [Nm/s], which is derived from:

$$\frac{d\omega_r}{dt} = J_g + \frac{J_t}{n_g^2} \quad (7)$$

J_g and J_{wt} are respectively rotational inerias of the generator rotor and the wind turbine rotor. ~~The~~ n_g is the gear ratio, which can be set 1 in case of direct drive system (without gearbox).

2.1.3. Pitch blade controller

The power output of wind turbine generator always fluctuates depending on wind speed variations and its power output is not allowed to exceed its rating capacity. Therefore, the pitch blade controller works to maintain rotor speed of the wind turbine not exceeding the permissible speed limit. The schematic diagram of pitch blade controller model is shown in Figure 5 [21]. The controller maintains the rotor speed of wind turbine (ω_r) not to exceed its reference value (ω_r*). The control loop of pitch actuator is represented by a first order transfer function with time constant T. PI controller is used to obtain pitch angle reference (β*).

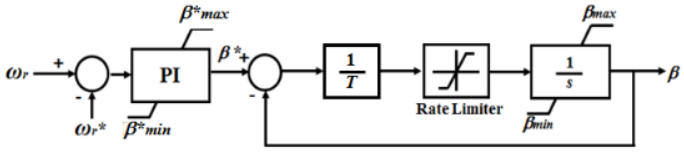

Figure 5. The pitch blade controller model.

2.2. Generator Model

For the generator model, permanent magnet synchronous machine model ~~presented~~ in the PSCAD/EMTDC master library is considered in this study. Voltage equations for main stator windings, voltage equations for the short-circuited windings, and flux linkage equations of the windings are represented in the *dq0* reference frame. A more detailed explanation about the generator in the PSCAD/EMTDC model can be found in [22, 23].

2.3. MMC System

2.3.1. Configuration and Operation of MMC

Configuration of the three phase MMC system is depicted in Figure 6. The MMC in this study is 7 (seven) levels modular converter. The MMC consists of three phase legs (Leg A, Leg B, and Leg C). The legs have two similar arms i.e., upper arm (p) and lower arm (n). Each arm consists of six identical sub-modules (SM), an arm inductor (L_{arm}), and an arm resistance (R_{arm}) arranged in series. The arm inductors are used to limit circulating arm current between three phase units and the valve short circuit current, and to contribute to interface between AC grid system and the MMC. The sub-module has two levels half bridge configuration composed of two IGBTs with anti-parallel diodes and a capacitor (C_{SM}). Three phase ac terminal voltage is connected to each phase leg on the common point connection between upper and lower arms through phase reactor consisting of an inductor (L_f) and a resistor (R_f). The reactor is used as a filter for AC voltage and current [24].

In the operation of the MMC, the DC link voltage (V_{dc}) charges the capacitor (C_{SM}) in the entire sub-module in which the sub-modules are switched into inserted state or bypassed state. In the inserted state, the sub-module capacitor can be charging or discharging depending on voltage reference polarity. The switching state of sub-module conditions is given in Table 1. Figures 7 shows the direction of sub-module arm current (I_{arm}) according to S1 and S2 switching state. The positive polarity of arm current direction is indicated in the red color, and negative polarity of arm current direction is indicated in the blue color.

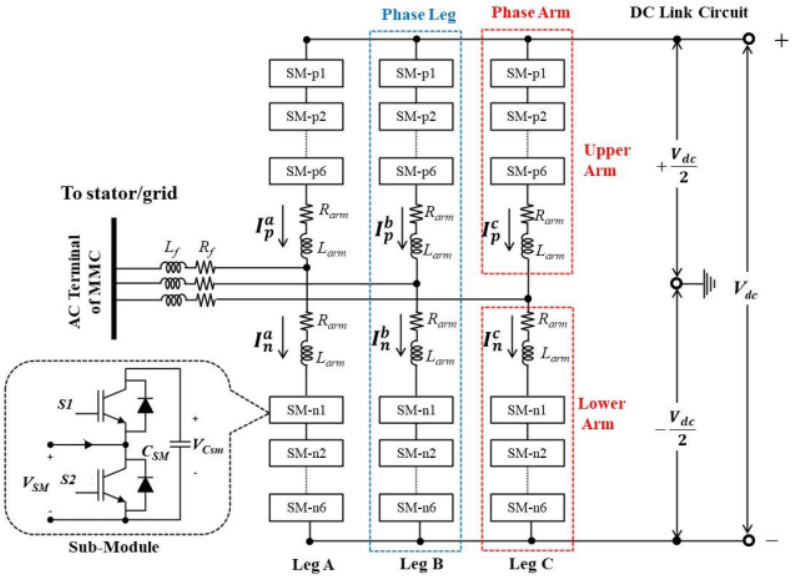

Figure 6. Configuration of MMC

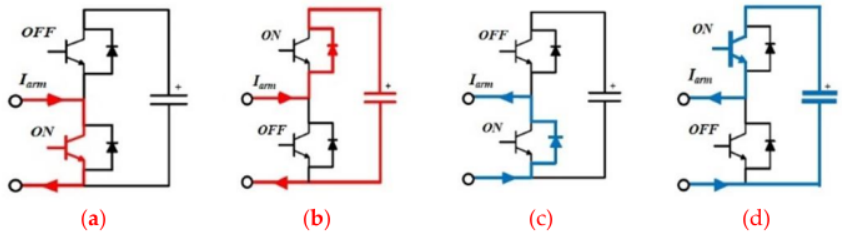

Figure 7. Current flow in sub-module according to switching state: (a) Bypass in positive polarity (b) Charging in positive polarity (c) Bypass in negative polarity (d) Discharging in negative polarity

Table 1. Switching state of the Sub-Module conditions

Switching State		Terminal Voltage of SM (V_{SM})	Arm Current Polarity	Status of Capacitor
S1	**S2**			
OFF	ON	0	+	Bypass
ON	OFF	Vc_{sm}	+	Charging
OFF	ON	0	-	Bypass
ON	OFF	Vc_{sm}	-	Discharging

2.3.2. Stator Side MMC Controller

Active power and reactive power output of PMSG is controlled by the stator side MMC controller. Three phase current and voltage of stator winding are transformed into the dq-axis components by using Park Transformation, where the position of rotor angle (θ) is obtained from the rotational speed of the PMSG. Detail of control scheme of the stator side MMC controller is shown in Figure 8. Active power and reactive power are controlled independently by the q-axis current component and the d-axis current component, respectively. The PI controllers adjust power loop and inner current loop controllers for each of the d-axis and the q-axis components. The generator (PMSG) usually operates in unity power factor operation in which the active power output (P_S) is set according to power reference (P_{ref}) tracking by MPPT circuit, and the reactive power output (Q_S) is set at zero. The outer power loop controller generates the dq-axis reference currents ($I_S^{*(dq)}$). The inner current loop controller generates the dq-axis reference voltages ($V_S^{*(dq)}$). By using the invers Park Transformation, the dq-axis reference voltages are transferred into sinusoidal three phase reference voltages (+/-$V_S^{*(abc)}$) in which the minus (-) and plus (+) indicate the reference signal for upper arm and lower arm, respectively. To increase tracking capability of the controllers, the cross-coupling cancellation ($\omega_r(L_{Sarm}/2+L_{Sf}+L_S^{(dq)})$ is added at the output of inner loop of current controller. $L_S^{(dq)}$ denotes the dq-axis components of leakage inductance of stator winding of the generator, L_{Sarm} and L_{Sf} denote the arm inductance and reactor inductance of Stator side MMC, respectively.

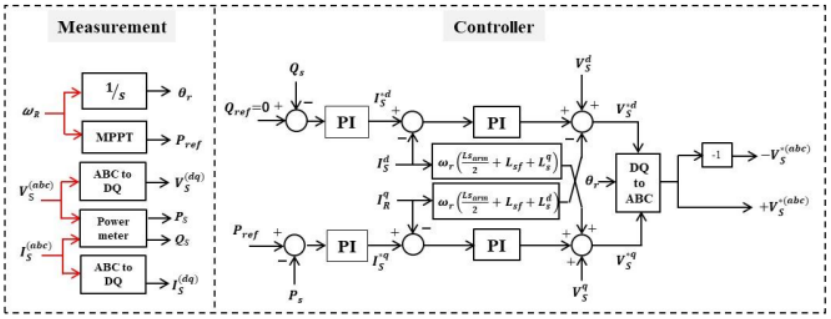

Figure 8. Stator Side MMC Controller

2.3.3. Grid Side MMC Controller

The control scheme of the grid side MMC controller is shown in Figure 9. The control loop is designed for controlling the DC link circuit voltage (V_{dc}), and the reactive power output of grid side MMC (Q_g) in a similar way to the stator side MMC based on the dq vector control. Three-phase currents ($I_G^{(abc)}$) and voltages ($V_G^{(abc)}$) at ac terminal of the grid side MMC are transformed into the dq-axis form by using Park Transformation, where the phase angle (θ_G) and angular frequency (ω_G) are obtained from Phase Locked Loop (PLL) controller. The PLL controller technique used in this study is referred to the original PSCAD/EMTDC's master library. The instantaneous active power (P_G) and reactive power

(Q_G) are calculated by using power meter, and the instantaneous rms voltage (V_G) of the ac terminal is obtained from the three phase rms voltmeter.

In the grid side MMC controller, the q-axis component (I_{Gq}) is used to control DC link circuit voltage at a constant DC voltage reference (V^*_{dc}), and the *d*-axis current component (I_{Gd}) is used to control reactive power output (Q_G) or the ac terminal voltage (V_G) of the grid side MMC. In normal mode operation, the reactive power reference (Q^*_G) is usually set at zero to maintain power factor at unity. In fault mode operation, the grid voltage reference (V^*_G) is set at 1.0 pu. During fault conditions, the grid side MMC controller will change its operation from normal mode to fault mode when the voltage at the terminal output drops below 80%. The PI control loop systems are also consisting of the inner current loop control and the power loop control for each of the *d*-axis and the *q*-axis components. The cross coupling in the term of $\omega_G(L_{Garm}/2+L_{Gf})$ is added to the output of the inner loop current control for the controller tracking improvement, where L_{Garm} and L_{Gf} are arm inductance and reactor inductance of Grid side MMC, respectively.

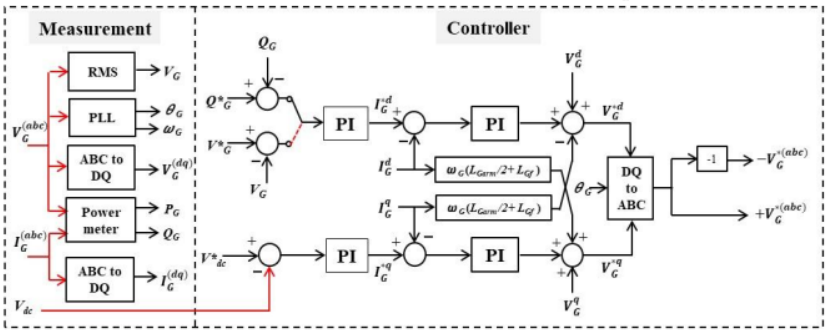

Figure 9. Grid Side MMC Controller

The aim of the development of the wind turbine generator models in this paper is to simulate and analyze the dynamic behaviors of grid connected wind farm in steady state and transient conditions. The grid connectivity study is an important requirement in the development stage of wind farm project. In order to improve dynamic performance of the control system of Stator Side MMC and Grid Side MMC, certainly the improvement methods such as energy-shaping L2-gain [25], sliding mode controller [26], pole and placement, etc, can be applied to the proposed model. However, because only concern in this study is grid connectivity study, hence the control system that applied to the Stator Side MMC and the Grid Side MMC can be standard control model by using PI controller. The gain control parameters such as *Kp* and *Ki* are obtained by using pole and placement method and optimum symmetrical criterion method for inner and outer controllers, respectively.

2.3.4. MMC Inner Control

As the MMC has three phase legs, a circulating current can exist within each phase leg. In addition, two arm configurations in the MMC can generate two different voltage levels for each sub-module in the same arm [27]. The circulation phase leg current should be eliminated, and each sub-module capacitor voltage should be kept balanced at same level. To handle these problems the MMC inner controller is introduced. The MMC inner controller depicted in Figure 10 is applied to both the stator side MMC and grid side MMC. The purpose of MMC inner controller is to control circulation current in the phase legs at zero, and to maintain each sub-module capacitor voltage at the same level. Average circulation current through a phase leg (I_{diff}) is obtained by adding the current through upper arm (I_p) and the current through lower arm (I_n) divided by 2. The circulating current reference for each phase leg is set at zero. The controller adjusts to impose the circulation voltage (V_{diff}) into the reference voltage for upper arm and the lower arm. To control voltage balancing of each SM capacitor extra controllers are required. Detailed

explanation for circulating current controller and the SM capacitor voltage balancing controller can be found in [28].

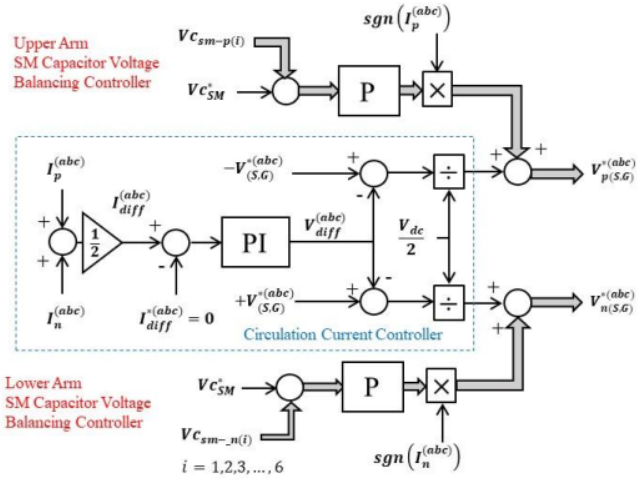

Figure 10. MMC Inner Controller

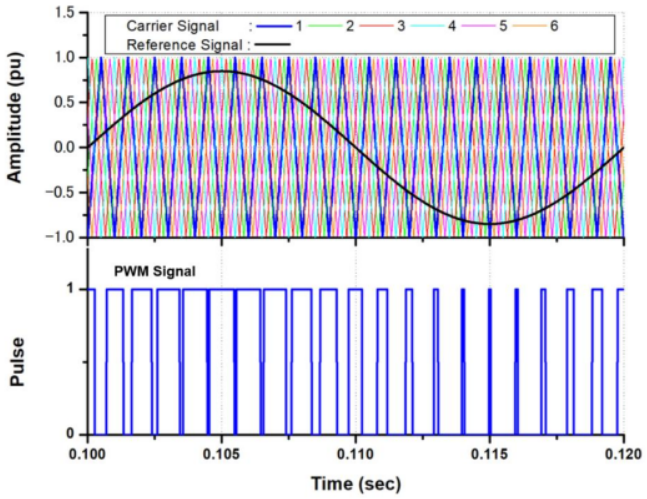

Figure 11. PS-PWM Technique

2.3.5. Phase Shifted Pulse Width Modulation (PS-PWM)

In general, modulation techniques for multilevel converter can be summarized in three categories: Multi Carrier Pulse Wave Modulation (MC-PWM), Nearest Level Modulation (NLM), and Space Vector Modulation (SVM) [29,30]. The multi-carrier Phase Shifted Pulse Wave Modulation (PS-PWM) technique is considered in this study due to its merits compared to other approaches. The PS-PWM technique is more effective and more superior in controlling the MMC, that is, the power distribution over entire sub-modules can be provided, and the voltage balance at sub-module capacitors can be achieved. Figure 11 shows the process of the PS-PWM technique. Each sub-module has an independent carrier signal in which the reference signal is distributed to all the series sub-modules in each leg. The goal of the modulation is to produce PWM signal for switch-

ing the IGBT gate on each sub-module. The number of the carrier signal applied is depending on the level of the MMC, and in this case, it is N-1, where N is the level of the MMC. The phase shift (ϕ) between the carrier signals can be obtained through $\phi = 360^{o}/(N-1)$ [31]. The frequency and amplitude of all carrier signals should be equal. As the SM capacitor voltage balancing controller is applied to each SM, the PS-PWM with individual capacitor voltage control technique [28] is considered.

2.4. DC link Circuit and Over Voltage Protection System

Figure 12 shows the DC link circuit model of back-to-back MMC converter. The circuit model consists of two dc link capacitors, a DC chopper, and an over voltage protection controller. The DC link circuit is a connection circuit which connects the stator side MMC and the grid side MMC. The dc voltage on the DC link circuit should be kept at constant at rated operating dc voltage so that the power flow from the generator to grid system can be achieved smoothly. When a disturbance such as a short circuit occurs in the grid system, the active power on the ac terminal of grid side MMC decreases, while the active power from the generator is still produced. This condition leads to significant increase of the DC link circuit voltage due to power unbalance between the stator side MMC and the grid side MMC. When the dc voltage is larger than 1.05 pu, the over voltage protection controller is activated, and then the active power from generator is absorbed by a chopper resistance (R_{ch}). Value of the resistance can be adjusted according to the amount of active power produced by the wind turbine generator which is represented by the reference power (P_{ref}).

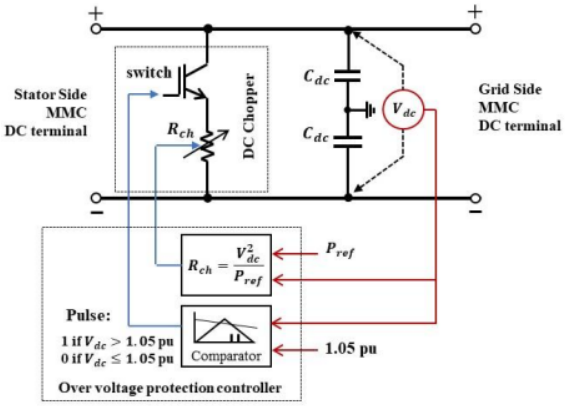

Figure 12. DC link Circuit model

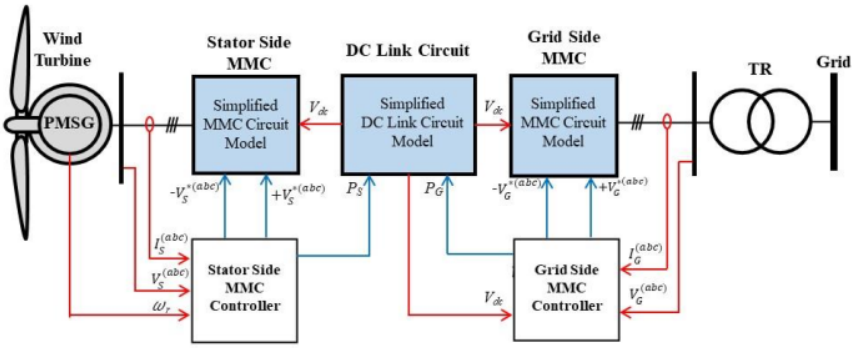

Figure 13. Average model configuration of the wind turbine generator

3. Average Model of MMC Controlled Wind Turbine Generator

The aim of the average model is to reduce the complexity and simulation time. Study of grid-connected wind farms with many generators becomes inefficient if the simulation is performed using the detailed model. In the average model, power electronic IGBTs of MMC circuit and switching phenomenon are neglected, and hence the model becomes simpler. Configuration of the average model of MMC controlled wind turbine generator is shown in Figure 13. The main part of the model consists of wind turbine generator including pitch controller system, stator side MMC with controller system, DC link circuit including over voltage protection, and grid side MMC with controller system. Wind turbine, drive train, pitch controller, and generator models are same as those used in the detailed model. Likewise, the stator side MMC controller and the grid side MMC controller are same as the controllers used in the detailed model. Only the MMC circuits and the DC link circuit are simplified. It should be noted that behavior of sub-module capacitor voltage is not considered in the average model. Therefore, the inner MMC controller can be omitted.

3.1. MMC Circuit Model

To derive a model representation of the MMC, the equivalent approach model as shown in Figure 14 is considered. By applying Kirchhoff Voltage Low (KVL) across the phase reactor, differential equations for three phase circuit can be expressed as follows [32, 33]:

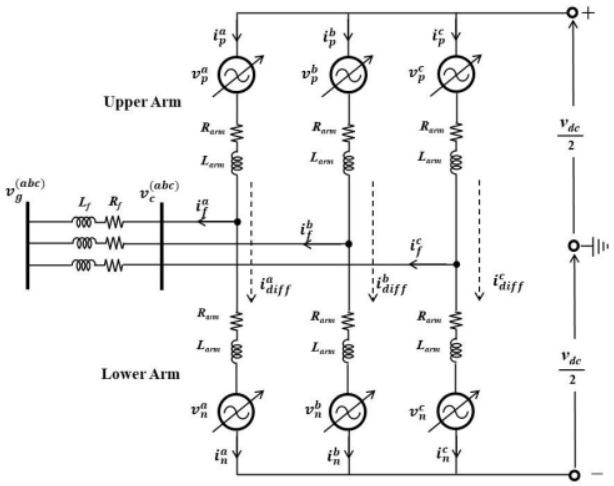

Figure 14. Electrical circuit model of MMC

$$L_f \frac{di_f^{(abc)}}{dt} = v_g^{(abc)} - v_c^{(abc)} - R_f i_f^{(abc)} \quad (8)$$

By applying Park Transformation, the three-phase differential equation in the *dq*-axis component can be expressed as follows:

$$L_f \frac{di_f^d}{dt} = v_g^d - v_c^d - R_f i_f^d + \omega_g L_f i_f^q \quad (9)$$

$$L_f \frac{di_f^q}{dt} = v_g^q - v_c^q - R_f i_f^q - \omega_g L_f i_f^d \quad (10)$$

The complex grid power (S_g) can be calculated as follows:

$$S_g = \left(v_g^d + jv_g^q\right)\left(i_f^d - ji_f^q\right) \Rightarrow S_g = \left(v_g^d i_f^d + v_g^q i_f^q\right) + j\left(v_g^q i_f^d - v_g^d i_f^q\right) \quad (11)$$

From (11) the active power and reactive power can be written as

$$P_g = v_g^d i_f^d + v_g^q i_f^q \quad (12)$$

$$Q_g = v_g^q i_f^d - v_g^d i_f^q \quad (13)$$

In the same way, active power and reactive power flow to the converter valve can be written as

$$P_c = v_c^d i_f^d + v_c^q i_f^q \quad (14)$$

$$Q_g = v_c^q i_f^d - v_c^d i_f^q \quad (15)$$

As reactive power does not propagate to the DC side of the converter valve, the DC current (i_{dc}) is obtained as regards to active power balance between AC side and DC side. By assuming that the losses on the converter can be omitted, the following relation can be written:

$$P_c = P_{dc} \Rightarrow v_c^d i_f^d + v_c^q i_f^q = v_{dc} i_{dc} \quad (16)$$

The voltages waveform at the AC side of the MMC depends on the reference voltages fed to each six arms. Inserted voltages in the six arms of MMC are represented by controlled voltage source. The upper and lower arm currents can be written as follows:

$$i_p^{(abc)} = i_{diff}^{(abc)} + \frac{i_f^{(abc)}}{2} \quad (17)$$

$$i_n^{(abc)} = i_{diff}^{(abc)} - \frac{i_f^{(abc)}}{2} \quad (18)$$

where i_{diff} is circulating phase leg current which can be determined as average of upper arm and lower arm currents as:

$$i_{diff}^{(abc)} = \frac{i_p^{(abc)} + i_n^{(abc)}}{2} \quad (19)$$

The voltage output at AC side of MMC is given by

$$v_c^{(abc)} = \frac{v_p^{(abc)} - v_n^{(abc)}}{2} - \frac{R_{am}}{2} i_f^{(abc)} - \frac{L_{am}}{2} \frac{di_f^{(abc)}}{dt} \quad (20)$$

The DC loop of each MMC arm can be expressed as

$$L_{arm} \frac{di_{diff}^{(abc)}}{dt} + R_{arm} i_{diff}^{(abc)} = \frac{v_{dc}}{2} - \frac{v_p^{(abc)} + v_n^{(abc)}}{2} \quad (21)$$

The inner difference voltage of each phase is given by

$$v_{diff}^{(abc)} = L_{arm} \frac{di_{diff}^{(abc)}}{dt} + R_{arm} i_{diff}^{(abc)} \quad (22)$$

The reference voltage of upper arm and lower arm for each phase can be written as follows:

$$v_{pref}^{(abc)} = \frac{v_{dc}}{2} - \frac{v_p^{(abc)} - v_n^{(abc)}}{2} - v_{diff}^{(abc)} \quad (23)$$

$$v_{nref}^{(abc)} = \frac{v_{dc}}{2} + \frac{v_p^{(abc)} - v_n^{(abc)}}{2} - v_{diff}^{(abc)} \quad (24)$$

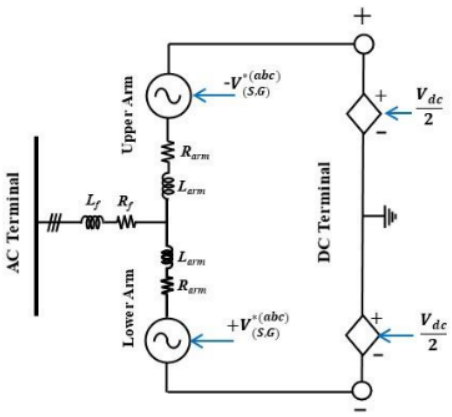

Figure 15. Simplified MMC circuit model

Referring to Figure 14, the proposed simplified MMC circuit model can be represented as depicted by Figure 15. The equivalent circuit for the MMC is represented by a pair of three phase ac voltage sources and a pair of dc voltage sources for upper arm and lower arm respectively. The ac voltage sources are connected to the MMC AC terminal through the arm inductor (L_{arm}), arm resistance (R_{arm}), reactor inductor (L_f), and reactor resistance (R_f). The series dc voltage sources are connected to the DC terminal of the MMC. ~~The~~ $-V_{S,G}^{(abc)}$ and $+V_{S,G}^{(abc)}$ are reference voltages for upper and lower arm respectively from the MMC controller. ~~The~~ $V_{dc}/2$ is used as reference voltage for the dc voltage sources, where ~~the~~ V_{dc} is voltage from the DC link circuit.

3.2. *DC Link Circuit Model*

Dynamic behavior of the capacitor voltage can be expressed by the following equation [32]:

$$\frac{dV_{dc}}{dt} = \frac{1}{C_{dc}V_{dc}}(P_S - P_G - P_{ch}) \quad (25)$$

where P_{ch} is power absorbed by chopper resistance.

In steady state condition, the DC link circuit voltage should be kept constant at rated voltage, and hence the power produced by the generator can be flowed to the grid. When a transient disturbance such as a short circuit occurs in the grid system, the DC link circuit voltage can exceed its rated voltage significantly because of unbalance of output power between the PMSG (P_S) and the grid side MMC (P_G). This phenomenon is important to consider in the grid connectivity study of wind farms. Therefore, the over voltage protection scheme is also included in the model. Configuration of the proposed DC link circuit model is shown in Figure 16. Power absorption by the chopper resistance is activated when the DC link voltage exceeds 1.05 pu.

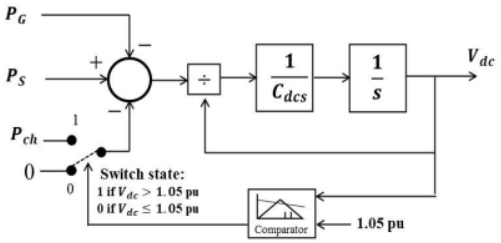

Figure 16. DC link circuit model

4. Simulation and Analysis

Figure 17 depicts the power system considered in the simulation study. A 50 MW wind farm is consisting of five 10 MW PMSG based wind turbines controlled by MMC system. The wind turbine generators (WTGs) are connected to each other by medium voltage collector power cables. Each collector power cable is represented by equivalent π circuit model. Power outputs from the wind turbine generators are collected at 33 kV main bus (B33), and then supplied to main grid through a 33kV/66kV main transformer and double circuit ~~of~~ 66 kV transmission line. Parameters of the PMSG and the MMC are presented in Tables 2 and 3, respectively.

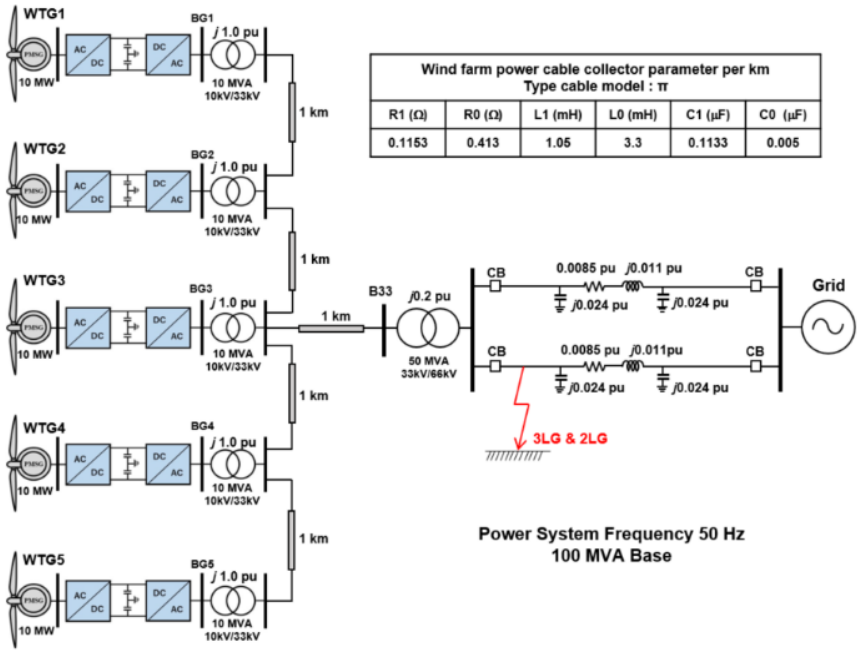

Wind farm power cable collector parameter per km Type cable model : π					
R1 (Ω)	R0 (Ω)	L1 (mH)	L0 (mH)	C1 (μF)	C0 (μF)
0.1153	0.413	1.05	3.3	0.1133	0.005

Figure 17. Power system model

Table 2. Parameters of PMSG

Parameter	Value	Parameter	Value
Rated MVA	10 MVA	Stator Winding Resistance	0.017 pu
Rated Voltage (L-L)	10 kV	Stator Leakage Reactance	0.0364
Rated Frequency	50 Hz	*d-axis* Unsaturated Reactance [X_d]	0.55 pu
Magnetic Strength	1.1 pu	*q-axis* Unsaturated Reactance [X_q]	1.11 pu

Table 3. Parameters of MMC

Parameter	Value	Parameter	Value
Rated Power	10 MVA	SM Capacitor	9.2 mF
Rated AC Voltage	10 kV	Arm Inductance	3.8 mH
Rated DC Voltage	18 kV	Arm Resistance	0.097 Ω
Number SMs per arm	6	Reactor Inductance	0.773 mH
Carrier Frequency	1000 Hz	Reactor Resistance	0.019 Ω
DC link Capacitor	7.4 mF		

The power system model shown in Figure 17 has been analyzed with the detailed and the average models by using ~~simulation~~ PSCAD/EMTDC. Accuracy of the average model has been validated by comparing its responses under both steady state and transient conditions with those obtained from the detailed model. The simulations have been performed on the personal computer (Intel (R) Core (TM) i7-9700 CPU @ 3.0 GHz Ram 64 GB.

4.1. Steady State Performance Analysis

In steady state study, natural wind velocity data measured in Hokkaido Island, Japan, are randomly selected for the simulation. The wind speed data of 300 seconds are applied to each wind turbine generator, and they are shown in Figure 18. In this paper, dynamic performances of all wind turbine generators are not shown, but only the dynamic performances of WTG1 are presented as a representative for all WTGs. The dynamic performances of WTG 1, such as rotor speed response, the voltage profile at terminal stator winding, active and reactive power output of the PMSG, the dc voltage profile at DC link circuit, active and reactive power output of grid side MMC, and voltage profile at low voltage side of the step-up transformer (Bus BG1), are presented in Figure 19. Total active power and reactive power output of the wind farm and voltage profile at Bus B33 are presented in Figure 20. In can be confirmed that, the dynamic performances of the WTG under steady state condition can be clearly analyzed in the detailed model and the average model representation, and good dynamic control performances can clearly be seen. It is clear that the average model has sufficient accuracy in steady state analysis. Moreover, the computation time of the average model is much shorter than that of the detailed model as presented in Table 4.

Table 4. Computation time of each model for 300 sec steady state analysis

Simulation	Computation Time	
	Detailed Model	Average Model
Time step	10 µsec	100 µsec
Duration	840 hours	11 minutes

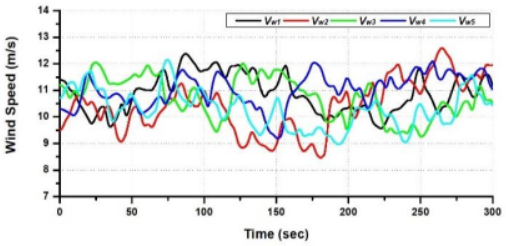

Figure 18. Wind velocity data

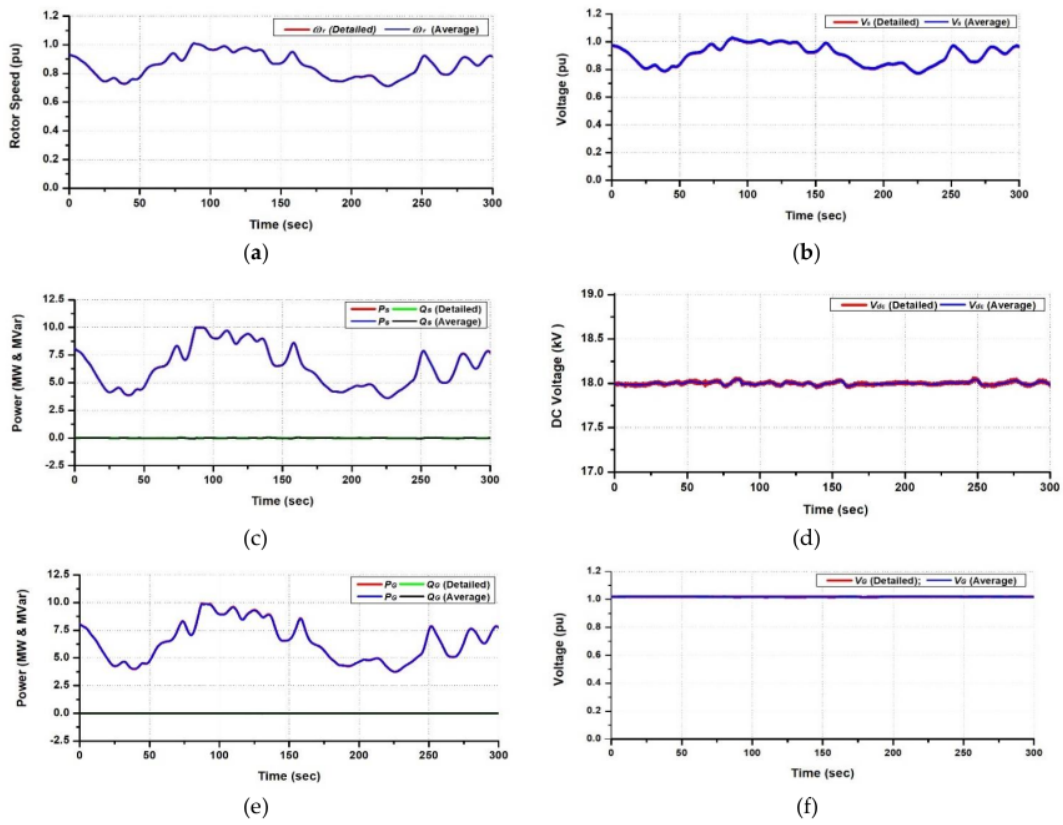

Figure 19. Dynamic Performances of WTG1 under steady state condition: (**a**) Rotor speed response; (**b**) Voltage profiles at terminal of stator winding; (c) Active and reactive power output of the PMSG; (d) DC link circuit voltage profile; (e) Active and reactive power output of grid side MMC; (f) Voltage profile at Bus BG1.

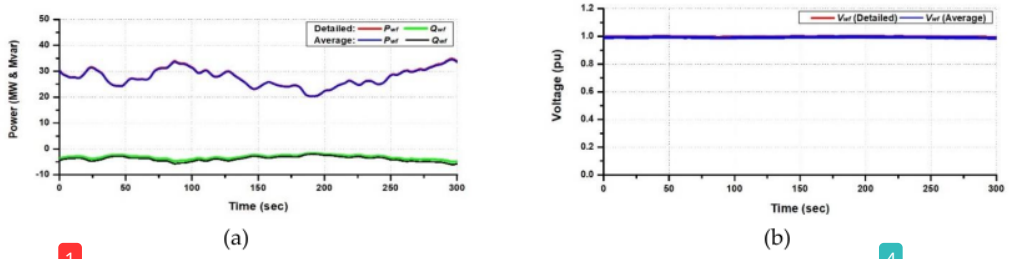

Figure 20. Power output and voltage performances of the wind farm under steady state condition: (**a**) Total active power and reactive power outputs of the wind farm; (**b**) Voltage profile at Bus B33.

4.2. Transient Performance Analysis

For transient performance study, a short circuit of three lines to ground fault (3LG) and two lines to ground fault (2LG) on one of the circuits of the 66-kV transmission line is considered as disturbance. The location of the faults is shown in Figure 17. The faults occur at 0.1, and then the circuit breakers (CBs) on the faulted line are opened at 0.2 sec to isolate the fault from the system. The CBs are reclosed at 1.0 sec on the assumption that the fault has been cleared. During the simulation time of 5 sec, the wind velocities of WTGs are assumed to be constant at rated velocity of 12 m/sec.

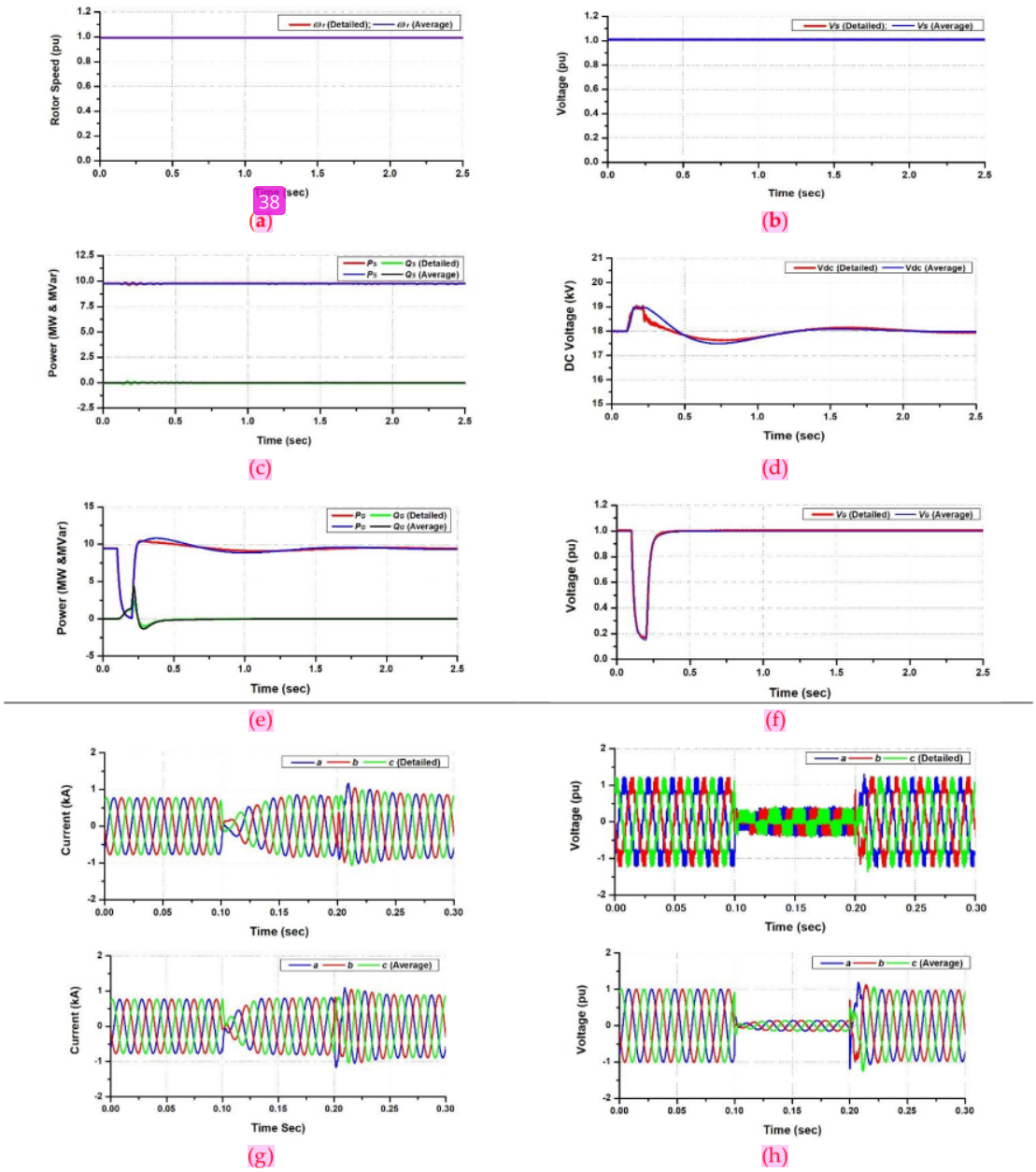

Figure 21. Dynamic performances of WTG1 in case of 3LG: (**a**) Rotor speed response; (**b**) Voltage profiles at terminal ~~output~~ of stator winding; (c) Active and reactive powers output of the PMSG; (d) DC-link circuit voltage profile; (e) Active and reactive power output of grid side MMC; (f) Voltage profile at Bus BG1; (g) Waveform of current at grid side MMC; (h) Waveform of voltage at grid side MMC.

433
434

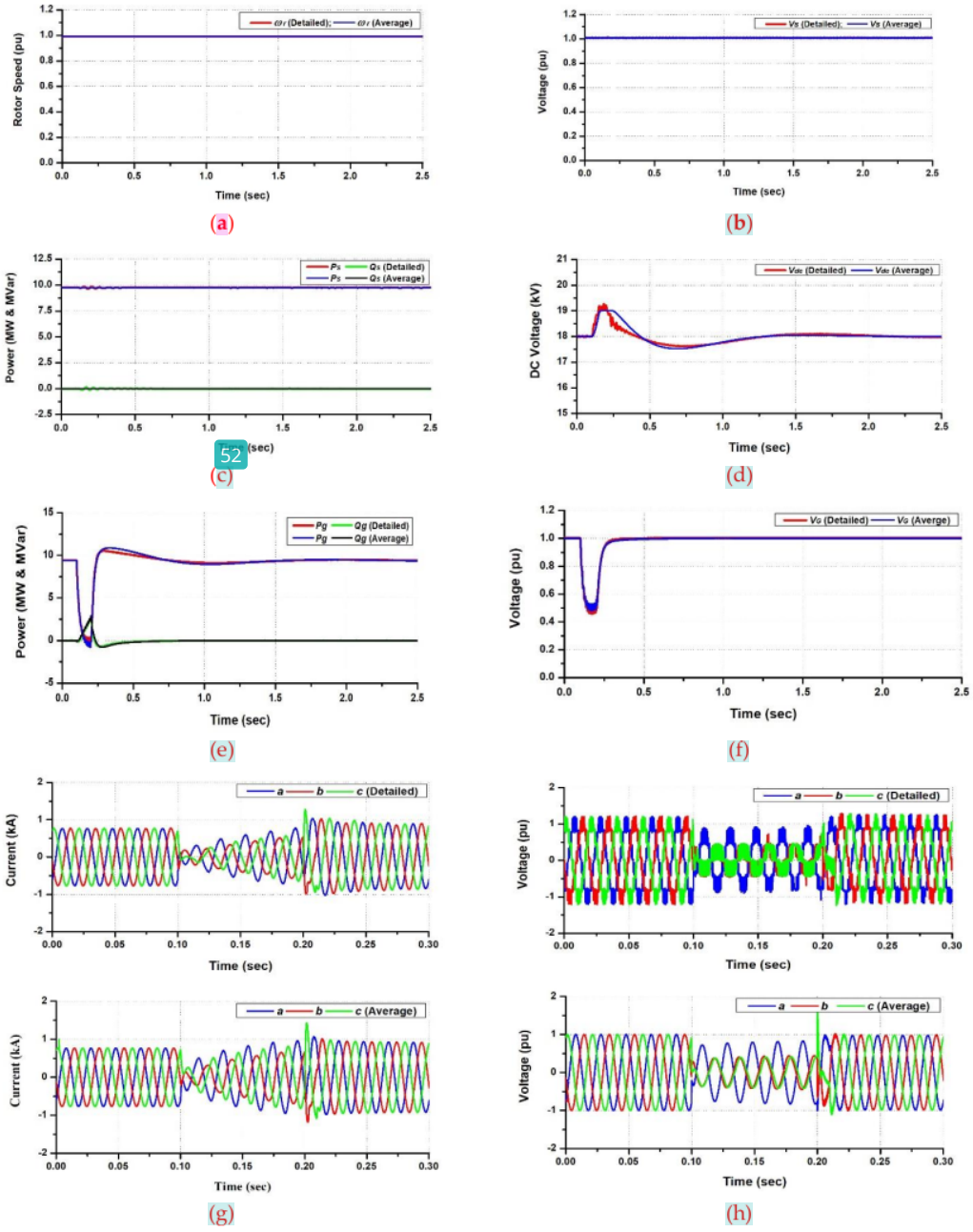

Figure 22. Dynamic Performance of WTG1 in case of 2LG: (**a**) Rotor speed response; (**b**) Voltage profiles at terminal output of stator winding; (c) Active and reactive power output of the PMSG; (d) DC link circuit voltage profile; (e) Active and reactive power output of grid side MMC; (f) Voltage profile at Bus BG1; (g) Waveform of current at grid side MMC; (h) Waveform of voltage at grid side MMC.

435
436
437

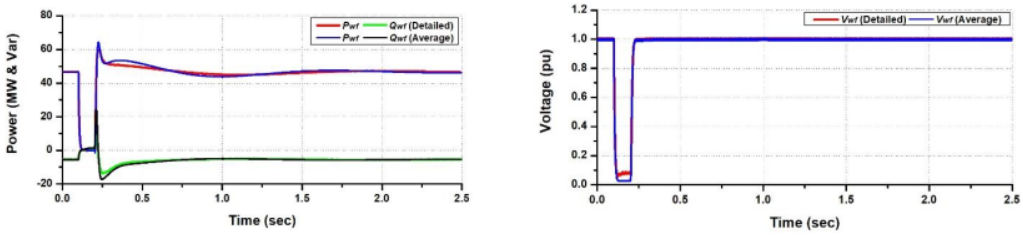

Figure 23. Power output and voltage performances of the wind farm at Bus B33 under 3LG case: (**a**) Active power output of wind farm; (**b**) Voltage profile at Bus B33.

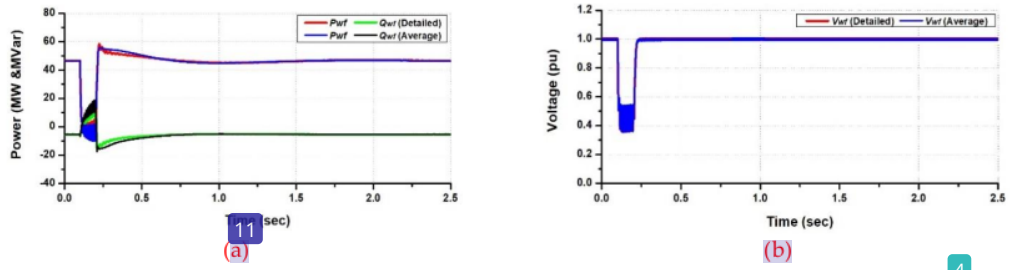

Figure 24. Power output and voltage performances of the wind farm at Bus B33 under 2LG Case: (**a**) Active power output of wind farm; (**b**) Voltage profile at Bus B33.

As the wind speed applied to each wind turbine generator is same, the dynamic performances of each individual WTG in the transient conditions for 3LG and 2LG are represented by the dynamic performances of only WTG1 as presented in Figures 21 and 22, respectively. As the wind turbine generator is totally decoupled from the grid network by back-to-back MMC, the short circuit on the grid network does not affect dynamic performances on the generator side in cases of 3LG and 2LG. The transient disturbances have almost no influence on the dynamic performances of the generator such as rotor speed response, power outputs and voltage profile. However, the transient disturbances affect ~~to~~ performances of the DC link circuit voltage, power output of Grid side MMC, current and voltage profiles at Bus BG1. In DC link circuit, the transient dc voltage appears due to the 3LG and 2LG faults, but it can be controlled by the over voltage protection system, and hence the dc voltage can be returned to the initial condition after the fault is cleared. It is also confirmed that the power output of Grid side MMC ~~performance~~ and voltage profile at Bus BG1 can be returned to the initial conditions after the fault. The performances of final power output of the wind farm and voltage profile at Bus 33 for 3LG and 2LG cases are shown in Figures 22 and 24, respectively.

From the simulation results, it can be confirmed that the dynamic performances of the detailed model and the average model have almost the same responses also in the transient condition. The different responses between the detailed and average models appear slightly in the DC link circuit voltage profile and the power output ~~characteristic~~ of Grid side MMC. However, they are slight and disappear after returning to the steady-state condition after fault clearance.

4.3. Discussion

The aim of the development of the wind turbine generator models in this paper is to simulate and analyze the dynamic behaviors of grid connected wind farm in steady state and transient conditions. To verify the accuracy of the proposed models, the simulation results should be validated by real field data. However, the real field data is not easy to access. In addition, the implementation of the MMC controlled PMSG based wind turbine

is a new topology concept of wind turbine generator that has not been realized practically yet. Therefore, the detailed model is presented in this study because its dynamic behavior is close to real field conditions. To get real system situation, the wind farm model ~~as~~ shown in Figure 17 is adopted and simulated as the proposed detailed model. As a consequence, the s~~i~~mulation ~~duration~~ took very long computation time.

It is very important to understand that the proposed average model is an approach method to approximate the detailed model by reducing complexity of MMC circuit, where some parts such as the switching phenomena, power electronic IGBTs of the submodules are neglected in the simulation. In the steady state analysis, ~~the performances of~~ both models have almost same responses. In a case of the transien~~t~~ condition with a short circuit fault, there are slight differences in the simulation results in the DC voltag~~e~~ response and the active and reactive power response overshoot between the detailed model and the average model after the CB is opened.

As real wind farm can consist of hundreds of wind turbine generators, the simulation study cannot be performed by the detailed model. To solve this problem the average model is presented in this paper. The average model can be used as individual or aggregated wind turbine generator models in simulation analyses.

5. Conclusions

Dynamic performances ~~analysis~~ of the proposed detailed and the proposed average models of grid connected MMC controlled permanent magnet wind turbine generator hav~~e~~ been investigated. Comparative analyses between the detailed and the average models have been performed for steady state and transient conditions and it has been confirmed that both models have almost the same dynamic responses and have a good controllability. Although both models can be used in the analysis of grid connected wind farms, each model can have different purposes in applications.

The proposed detailed model is required a small discrete time step because power electronics IGBTs and their switching phenomena are considered. The detailed model is suited for analyzing the dynamic performance in control system design of an individual wind turbine generator in a short time simulation. The dynamic performance of MMC's sub-modules and harmonics analyses can be handled by the detailed model.

In the proposed average model, power electronics IGBTs converter and switching phenomena are omitted, and thus the simulation time step can be much larger than that of the detailed model. The model can be used as individual or aggregated model of the wind turbine generators and wind farm. The model is suited to analyze a power system with many wind generators which cannot be analyzed by using the detailed model.

In the near future, the development of control strategies to improve dynamic performance of the MMC in controlling the power flow from the generator to the grid system would be performed. Improvement of gain control by adopting linear or nonlinear methods would be one of the key point in the next research. Optimization methods based on Artificial Intelligence (AI) will also be considered in the future research.

Appendix

In this paper, it should be noted that a 3-phase *abc* to *dq*0 transformation as well as its inverse are used, and they are expressed by the following equations [16]:

Park Transformation

$$\begin{bmatrix} d \\ q \\ 0 \end{bmatrix} = \frac{2}{3}\begin{bmatrix} \cos(\theta) & \cos\left(\theta - \frac{2\pi}{3}\right) & \cos\left(\theta + \frac{2\pi}{3}\right) \\ \sin(\theta) & \sin\left(\theta - \frac{2\pi}{3}\right) & \sin\left(\theta + \frac{2\pi}{3}\right) \\ \frac{1}{2} & \frac{1}{2} & \frac{1}{2} \end{bmatrix}\begin{bmatrix} a \\ b \\ c \end{bmatrix} \quad (26)$$

Invers Park Transformation

$$\begin{bmatrix} a \\ b \\ c \end{bmatrix} = \frac{2}{3}\begin{bmatrix} \cos(\theta) & \sin(\theta) & 1 \\ \cos\left(\theta - \frac{2\pi}{3}\right) & \sin\left(\theta - \frac{2\pi}{3}\right) & 1 \\ \cos\left(\theta + \frac{2\pi}{3}\right) & \sin\left(\theta + \frac{2\pi}{3}\right) & 1 \end{bmatrix}\begin{bmatrix} d \\ q \\ 0 \end{bmatrix} \quad (27)$$

Author Contributions

Conceptualization: M.R. and J.T; Software: M.R; Supervision: A.U., R.T., and J.T.; Validation: A.U., R.T., and J.T; Writing – original draft: M.R and J.T.
All authors have read and agreed to the published version of the manuscript.

Funding

This work was supported in part by the Japan Society for the Promotion of Science

Conflicts of Interest:

The authors declare no conflict of interest.

References

1. Vestas to Launch Giant 15 MW Offshore Wind Turbine. Available online: https://www.oedigital.com/news/485191-vestas-to-launch-giant-15mw-offshore-wind-turbine (accessed on 10 February 2021)
2. Wind power experts expect wind energy costs to decline up to 35% by 2035. Available online: https://www.renewableenergyworld.com/wind-power/wind-power-experts-expect-wind-energy-costs-to-decline-up-to-35-by-2035/#gref (accessed on 15 April 2021)
3. Jiangchai Qin, J.Q.; Maryam Saeedifard, M.S.; Andrew Rockhill, A.R.; Rui Zhou, R.Z. Hybrid design of modular multilevel converters for HVDC systems based on various submodule circuits, *IEEE Transaction on Power Delivery* **2015**, *30*, 385–394.
4. Xiaojie Shi, X.S.; Zhiqiang Wang, Z.W.; Bo Liu, B.L.; Yiqi Liu, Y.L.; Leon M. Tolbert, L.M.T; Fred Wang, F.W. Characteristic investigation and control of a modular multilevel converter-based HVDC system under single-line-to-ground fault conditions, *IEEE Transaction on Power Electron* **2015**, *30*, 408–421.
5. A Lesnicar, A. L; Rainer Maquardt, R.M. An innovative modular multilevel converter topology suitable for a wide power range, Proceeding of 2003 Power Tech Conference, Bologna, Italy, 23-26 June 2003.
6. Zicong Zhang, Z.Z.; Junghun Lee, J.L; Gilsoo Jang, G.J. Improved control strategy of MMC-HVDC to improve frequency support of AC system. *Applied Sceinces* **2020**, *10*, 7282. https://doi.org/10.3390/app10207282
7. Nusrat Husain, N.H; Syed M. Usman Ali. S.U.A. On integration of wind power into existing grids via Modular Multilevel Converter based HVDC Systems. *International Journal of Renewable Energy Research* **2020**, *10*, https://doi.org/10.20508/ijrer.v10i3.10638.g7980.
8. Jingyi Li. J.L; Xiaohe Wang, X.W.; Jing Lyu. J.L.; Haoxiang Zong, H.Z.; Tao Xue, T.X.; Zixi Fang. Z.F.; Xu Cai, X.C. Stability analysis of wind farm connected to hybrid HVDC converter. Proceeding of 2020 IEEE 9th International Power Electronics and Motion Control Conference (IPEMC2020-ECCE Asia), Nanjing, China, 29 Nov-2 Dec 2020.
9. Md Ismail Hossain, M.I.H; Mohammad A. Abido, M.A.A. Positive-Negative Sequence Current Controller for LVRT Improvement of Wind Farms Integrated MMC-HVDC Network," *IEEE Access* 2020, *8*, 193314-193339.
10. Yingbiao Li, Y.L.; Jianbo Guo, J.G.; Xi Zhang, X.Z.; Shanshan Wang, S.W.; Shicong Ma, S.M.; Bing Zhao, B.Z.; Guanglu Wu, G.W.; Tiezhu Wang, T.W. Over-voltage suppression methods for the MMC-VSC-HVDC wind farm integration system. *IEEE Transactions on Circuits and Systems II: Express Briefs* **2020**, *67*, 355-359.
11. Liudmila Popova, L.P; Ke Ma, K.M; Frede Blaabjerg, F. B.; Juha Pyrhonen, J.P. Device loading of a modular multilevel converter in wind power. *IEEJ Journal of Industry Applications* **2014**, *4*, 380-386.
12. Weide Guan, W.G; Shoudao Huang, S.H; Xiaoqing Huang, X.H. Medium-voltage wind generation system based on MPMSG and MMC and its fault-tolerant," Proceeding of 2019 IEEE 3rd International Electrical and Energy Conference (CIEEC), Beijing, China, 7-9 Sept 2019.
13. Salman K. Salman, S.K; Anita L.J. Teo, A.T. Windmill modeling consideration and factors influencing the stability of a grid-connected wind power-based embedded generator. *IEEE Trans. Power System* **2003**, *18*, 793–802.
14. N. Dizdarevic, N.D; M. Majstrovic, M.M; S. Zutobradic, S.Z. Power quality in a distribution network after wind power plant connection. Proceeding of IEEE PES Power System Conference and Exposition, New York, USA, 10-13 Oct. 2004.
15. A new era in direct drive generator design. Available online: https://www.lagerwey.com/technology/generator/ (accessed on 5 Dec 2021)

16. Soichiro Kiyoki, S.K; Kiyoshi Sakamoto, K.S; Hiramu Kakuya, H.K.; Mitsuru Saeki, M.S. 5-MW downwind wind turbine demonstration and work toward smart operation control. *Hitachi Review* **2017**, *66*, Available online: https://www.hitachi.com/rev/archive/2017/r2017_05/R5-02/index.html (accessed on 5 Dec 2021)
17. E-160 EP5, Available online: https://www.enercon.de/en/products/ep-5/e-160-ep5/ (accessed on 5 Dec 2021)
18. Siegfried Heier, *Grid integration of wind energy conversion system*, John Wiley & Sons Ltd: USA, 1998: pp.
19. S. M. Muyeen, S.M.M; Rion Takahashi, R.T.; Toshiaki Murata, T.M.; Junji Tamura, J.T. A variable speed wind turbine control strategy to meet wind farm grid code requirements. *IEEE Transaction on Power System* **2010**, *25*, 331-340.
20. Mingyan Yin, M.Y.; Chengyong Zhao, C.Z. Modeling of the wind turbine with a permanent magnet synchronous generator for integratin. Proceeding of IEEE Power Engineering Society General meeting, Tampa Florida, USA, 24-28 June 2007.
21. F. M. Gonzales-Longat, F.M.G; P. Wall, P.W; V. Terzija, V.T. A simplified model for dynamic behavior of permanent magnet synchronous generator for direct drive wind turbine. Proceeding of IEEE Trondheim PowerTech, Trondheim, Norway, 19-23 June 2011.
22. PSCAD/EMTDC Master Library Model, Manitoba HVDC Research Center, Canada 1994.
23. Permanent Magnet Machine Available online: https://www.pscad.com/knowledge-base/article/293 (accessed on 28 Sept 2018)
24. Guide for Electromagnetic transient studies involving VSC converter. CIGRE Technical Brochure Reference 832, April 2021
25. Penghan Li, P.L; Linyun Xiong, L.X.; Meiling Ma, M.M; Sunhua Huang, S.H; Zean Zhu, Z.Z.; Ziqiang Wang, Z.W. Energy-shaping L2-gain controller for PMSG wind turbine to mitigate sub synchronous interaction. *International Journal of Electrical Power and Energy Systems* 2021, 135, 107571 https://doi.org/10.1016/j.ijepes.
26. Penghan Li, P.L.; Linyun Xiong, L.X.; Fei Wu, F.W.; Meiling Ma, M.M; Jie Wang, J.W. Sliding mode controller based on feedback linearization for damping of sub-synchronous control interaction in DFIG-based wind power plants. *International Journal of Electrical Power and Energy Systems* 2019, *107, 239-250* https://doi.org/10.1016/j.ijepes.
27. Artjoms Timofejevs, A.T.; Daniel Gamboa, D.G. Control of MMC in HVDC Applications, Master thesis, Department of Energy Technology, Aalborg University, Denmark, 2013.
28. Rosheila Darus, R.D.; Georgios Konstantinou, G.K.; Josep Pou, J.P.; Salvador Ceballos, S.C.; Vassilios G. Agelidis, V.G.A. Comparison of phase-shifted and level-shifted PWM in the modular multilevel converter, Proceeding of IEEE International Power Electronics Conference (IPEC – ECCE Asia), Hiroshima, Japan, 18 - 21 May 2014.
29. R. Marquardt, R.M. Modular Multilevel Converter: An universal concept for HVDC-networks and extended DC-Bus-applications, Proceeding of The 2010 International Power Electronics Conference -ECCE ASIA-, Sapporo, Japan, 21-24 June 2010.
30. Joachim Holtz, J.H. Pulse width modulation-a survey, Proceeding of 23rd Annual IEEE Power Electronics Specialists Conference, Toledo, Spain, 29 Jun – 3 Jul 1992.
31. Leopoldo G. Franquelo, L.G.F.; Jose Rodriguez, J.R.; Jose I. Leon, J.I.L; Samir Kouro, S.K.; Ramon Portillo, R.P.; Maria A.M. Prats, M.A.M.P. The age of multilevel converters arrives, *IEEE Industrial Electronics Magazine* **2008**, *2*, 28-39.
32. Georgios Stamatiou, G.S. Analysis of VSC-based HVDC systems. Doctoral Thesis, Department of Energy and Environment, Division of Electric Power Engineering, Chalmers University of Technology, Gothenburg, Sweden, 2016.
33. Rostan Rodrigues, R.R.; Jun Li, J.L.; Herbert L. Ginn, H.L.G. A novel frequency domain control method for modular multilevel converters under non-sinusoidal supply conditions, Proceding of 2017 IEEE Energy Conversion Congress and Exposition (ECCE), Cincinnati, OH, USA, 1-5 Oct 2017.
34. L. M. Fernandes, L.M. F; C. A. Garcia, C.A.G.: F. Jurado, F.J. Operating capability as a PQ/PV node of a direct-drive wind turbine based on a permanent magnet synchronous generator, *Journal of Renewable Energy* **2010**, *35*, 1308-1318.

21Applied Sciences_Marwan2_rev1.docx

オリジナリティーレポート

27%
類似性指標

一次ソース

1	Marwan Rosyadi, Atsushi Umemura, Rion Takahashi, Junji Tamura, Noriyuki Uchiyama, Kazumasa Ide. "Simplified Model of Variable Speed Wind Turbine Generator for Dynamic Simulation Analysis", IEEJ Transactions on Power and Energy, 2015 Crossref	255 語 — 3%
2	kitami-it.repo.nii.ac.jp インターネット	248 語 — 3%
3	Marwan Rosyadi, Atsushi Umemura, Rion Takahashi, Junji Tamura. "A Study on Modular Multilevel Converter based Wind Turbine Generator Connected to Medium Voltage DC Collection Network", 2020 2nd International Conference on Broadband Communications, Wireless Sensors and Powering (BCWSP), 2020 Crossref	162 語 — 2%
4	Ide, K., N. Uchiyama, J. Tamura, R. Takahashi, A. Umemura, and M. Rosyadi. "A New Simple Model of Wind Turbine Driven Doubly-fed Induction Generator for Dynamic Analysis of Grid Connected Large Scale Wind Farm", 3rd Renewable Power Generation Conference (RPG 2014), 2014. Crossref	124 語 — 2%
5	Eugeniusz Koda, Anna Miszkowska, Anna Sieczka. "Levels of Organic Pollution Indicators in Groundwater	117 語 — 1%

at the Old Landfill and Waste Management Site", Applied Sciences, 2017
Crossref

6	clok.uclan.ac.uk インターネット	70 語 — 1%
7	www.mdpi.com インターネット	66 語 — 1%
8	"Handbook of Wind Power Systems", Springer Science and Business Media LLC, 2013 Crossref	57 語 — 1%
9	Marwan Rosyadi, Atsushi Umemura, Rion Takahashi, Junji Tamura, Shin'ichi Kondo, Kazumasa Ide. "Development of phasor type model of PMSG based wind farm for dynamic simulation analysis", 2015 IEEE Eindhoven PowerTech, 2015 Crossref	57 語 — 1%
10	S. M. Muyeen. "Application of energy capacitor system to wind power generation", Wind Energy, 07/2008 Crossref	40 語 — 1%
11	res.mdpi.com インターネット	40 語 — 1%
12	ousar.lib.okayama-u.ac.jp インターネット	29 語 — < 1%
13	Marwan Rosyadi, S. M. Muyeen, Rion Takahashi, Junji Tamura. "Low voltage ride-through capability improvement of wind farms using variable speed permanent magnet wind generator", 2011 International Conference on Electrical Machines and Systems, 2011 Crossref	27 語 — < 1%

14	Hongbin Wu, Shuzhao Wang, Bo Zhao, Chengzhi Zhu. "Energy management and control strategy of a grid-connected PV/battery system", International Transactions on Electrical Energy Systems, 2015 Crossref	26 語 — < 1%
15	Smart Innovation Systems and Technologies, 2012. Crossref	26 語 — < 1%
16	Vijay Vittal, Raja Ayyanar. "Grid Integration and Dynamic Impact of Wind Energy", Springer Science and Business Media LLC, 2013 Crossref	26 語 — < 1%
17	"Object Tracking with LiDAR: Monitoring Taxiing and Landing Aircraft", Applied Sciences, 2018 Crossref	23 語 — < 1%
18	L. Sartika, M. Rosyadi, A. Umemura, R. Takahashi, J. Tamura. "Stabilization of PMSG based Wind Turbine under Network Disturbance by using New Buck Controller System for DC-Link Protection", 5th IET International Conference on Renewable Power Generation (RPG) 2016, 2016 Crossref	23 語 — < 1%
19	cyberleninka.org インターネット	22 語 — < 1%
20	www.koreascience.or.kr インターネット	22 語 — < 1%
21	manualzz.com インターネット	20 語 — < 1%
22	vbn.aau.dk インターネット	20 語 — < 1%

23	Chaudhary, Malati. "Investigating short circuit models for wind turbine generators.", Proquest, 2014. ProQuest	18 語	< 1%
24	Zhu, Ying, Ming Cheng, Wei Hua, and Wei Wang. "A Novel Maximum Power Point Tracking Control for Permanent Magnet Direct Drive Wind Energy Conversion Systems", Energies, 2012. Crossref	18 語	< 1%
25	"Stability Augmentation of a Grid-connected Wind Farm", Springer Nature, 2009 Crossref	17 語	< 1%
26	webfiles.portal.chalmers.se インターネット	17 語	< 1%
27	Rostan Rodrigues, Jun Li, Herbert L. Ginn. "A novel frequency domain control method for modular multilevel converters under non-sinusoidal supply conditions", 2017 IEEE Energy Conversion Congress and Exposition (ECCE), 2017 Crossref	16 語	< 1%
28	backend.orbit.dtu.dk インターネット	16 語	< 1%
29	Ming Yin, Gengyin Li, Ming Zhou, Guoping Liu, Chengyong Zhao. "Study on the control of DFIG and its responses to grid disturbances", 2006 IEEE Power Engineering Society General Meeting, 2006 Crossref	15 語	< 1%
30	Rajin M. Linus, Perumal Damodharan. "Wind Velocity Sensorless Maximum Power Point Tracking Algorithm in Grid-connected Wind Energy Conversion System", Electric Power Components and Systems, 2015	15 語	< 1%

Crossref

31	Kenta Koiwa, Koyo Inoo, Tadanao Zanma, Kang-Zhi Liu. "Virtual Voltage Control of VSG for Over-Current Suppression Under Symmetrical and Asymmetrical Voltage Dips", IEEE Transactions on Industrial Electronics, 2021 Crossref	13 語 — < 1%
32	core.ac.uk インターネット	12 語 — < 1%
33	etheses.whiterose.ac.uk インターネット	12 語 — < 1%
34	Teja Bandaru, Tanmoy Bhattacharya, Dheeman Chatterjee. "Unequal damping of the average sub-module capacitor voltages in modular multilevel converters", 2017 IEEE Applied Power Electronics Conference and Exposition (APEC), 2017 Crossref	11 語 — < 1%
35	digitalcommons.fiu.edu インターネット	11 語 — < 1%
36	hdl.handle.net インターネット	11 語 — < 1%
37	ieeexplore.ieee.org インターネット	11 語 — < 1%
38	mspace.lib.umanitoba.ca インターネット	11 語 — < 1%
39	Abdulrazig Alarabi, M. El-Hawary. "Multidimensional Optimal Control of wind Turbine Generator", 2014 IEEE Electrical Power and Energy Conference, 2014 Crossref	10 語 — < 1%

40 Chen, Xiaoqing. "Protection Scheme of an Integrated Photovoltaic and Type 3 Wind Turbines System.", University of Idaho, 2020
ProQuest
10 語 — < 1%

41 Kenta Koiwa, Yinqxiao Li, Kang-Zhi Liu, Tadanao Zanma, Junji Tamura. "Full Converter Control for Variable-Speed Wind Turbines Without Integral Controller or PLL", IEEE Transactions on Industrial Electronics, 2020
Crossref
10 語 — < 1%

42 Ko, H.S.. "Modeling and control of DFIG-based variable-speed wind-turbine", Electric Power Systems Research, 200811
Crossref
10 語 — < 1%

43 Shijie Chen. "Study on Control Method of Voltage Source Power Conditioning System for SMES", 2005 IEEE/PES Transmission &amp Distribution Conference &amp Exposition Asia and Pacific, 2005
Crossref
10 語 — < 1%

44 Zhou Yuebin, Jiang Daozhuo, Guo Jie, Hu Pengfei, Lin Zhiyong. "Control of Modular Multilevel Converter Based on Stationary Frame under Unbalanced AC System", 2012 Third International Conference on Digital Manufacturing & Automation, 2012
Crossref
10 語 — < 1%

45 www.hindawi.com
インターネット
10 語 — < 1%

46 Bin Jiang, Yanfeng Gong. "Arm Overcurrent Analysis and Calculation of MMC-HVDC System with DC-link Pole-to-Pole Fault", Electric Power Components and Systems, 2018
Crossref
9 語 — < 1%

47 Cleiton M. Freitas, Edson H. Watanabe, Luis F. C. Monteiro. "Grid-Forming MMC: A Comparison Between Single- and Dual-Loop Control Approaches", 2021 Brazilian Power Electronics Conference (COBEP), 2021
Crossref
9 語 — < 1%

48 F. Zhang, C. Yin, C. Hong, X. Yang, Y. Liu, X. Xie. "Frequency-dependent gain based damping control of SSO in wind farms connected to MMC-HVDC", The 16th IET International Conference on AC and DC Power Transmission (ACDC 2020), 2021
Crossref
9 語 — < 1%

49 Lee, Seungyong. "Improvement of Stability of a Grid-Connected Inverter with an LCL Filter by Robust Strong Active Damping and Model Predictive Control", University of Arkansas, 2021
ProQuest
9 語 — < 1%

50 Mihaela M. Grantcharova, Juan Carlos Fernández-Caliani. "Soil Acidification, Mineral Neoformation and Heavy Metal Contamination Driven by Weathering of Sulphide Wastes in a Ramsar Wetland", Applied Sciences, 2021
Crossref
9 語 — < 1%

51 MyeongSeok Kang, KyungMin Jin, JinHong Ahn, Eel-Hwan Kim. "Analysis of power quality in Jeju island power grid with STATCOM", 2011 International Conference on Electrical Machines and Systems, 2011
Crossref
9 語 — < 1%

52 da.qcri.org
インターネット
9 語 — < 1%

53 documents.mx
インターネット
9 語 — < 1%

54	eprints.whiterose.ac.uk インターネット	9 語 — < 1%
55	file.scirp.org インターネット	9 語 — < 1%
56	ijsrset.com インターネット	9 語 — < 1%
57	koreascience.or.kr インターネット	9 語 — < 1%
58	strathprints.strath.ac.uk インターネット	9 語 — < 1%
59	vtechworks.lib.vt.edu インターネット	9 語 — < 1%
60	www.coursehero.com インターネット	9 語 — < 1%
61	www.semanticscholar.org インターネット	9 語 — < 1%
62	Babak Badrzadeh. "Enhancement of fault ride-through capability and damping of torsional oscillations for a distribution system comprising induction and synchronous generators", 2009 IEEE PES/IAS Conference on Sustainable Alternative Energy (SAE), 09/2009 Crossref	8 語 — < 1%
63	E. U. Ubeku. "Wind energy conversion system- wind turbine modeling", 2008 IEEE Power and Energy Society General Meeting - Conversion and Delivery of Electrical Energy in the 21st Century, 07/2008 Crossref	8 語 — < 1%

64 Fujin Deng, Qiang Yu, Qingsong Wang, Rongwu Zhu, Xu Cai, Zhe Chen. "Suppression of DC-Link Current Ripple for Modular Multilevel Converters Under Phase-Disposition PWM", IEEE Transactions on Power Electronics, 2020
Crossref
8 語 — < 1%

65 Fujin Deng, Zhe Chen. "A new structure based on cascaded multilevel converter for variable speed wind turbine", IECON 2010 - 36th Annual Conference on IEEE Industrial Electronics Society, 2010
Crossref
8 語 — < 1%

66 Hamed H. Aly, M. E. El-Hawary. "An overview of offshore wind electric energy resources", CCECE 2010, 2010
Crossref
8 語 — < 1%

67 Islam, Thouhidul. "Application of Modular Multilevel Converters (MMC) Using Phase-Shifted PWM and Selective Harmonic Elimination in Distribution Systems.", University of Arkansas, 2018
ProQuest
8 語 — < 1%

68 Kan Liu, Z. Q. Zhu. "Position Offset-Based Parameter Estimation for Permanent Magnet Synchronous Machines Under Variable Speed Control", IEEE Transactions on Power Electronics, 2015
Crossref
8 語 — < 1%

69 M. Rosyadi, S. M. Muyeen, R. Takahashi, J. Tamura. "Transient stability enhancement of variable speed permanent magnet wind generator using adaptive PI-Fuzzy controller", 2011 IEEE Trondheim PowerTech, 2011
Crossref
8 語 — < 1%

70 Penghan Li, Linyun Xiong, Ziqiang Wang, Meiling Ma, Jie Wang. "Fractional - order sliding mode control for
8 語 — < 1%

damping of subsynchronous control interaction in DFIG - based wind farms", Wind Energy, 2019
Crossref

71 Qiang Song, Rong Zeng, Zhanqing Yu, Wenhua Liu, Yulong Huang, Wenbo Yang, Xiaoqian Li. "A Modular Multilevel Converter Integrated with DC Circuit Breaker", IEEE Transactions on Power Delivery, 2018 — 8 語 — < 1%
Crossref

72 Sixing Du, Apparao Dekka, Bin Wu, Navid Zargari. "Modular Multilevel Converter Based Medium-Voltage Motor Drives", Wiley, 2018 — 8 語 — < 1%
Crossref

73 docshare.tips — 8 語 — < 1%
インターネット

74 recercat.cat — 8 語 — < 1%
インターネット

75 vdocuments.mx — 8 語 — < 1%
インターネット

76 vsip.info — 8 語 — < 1%
インターネット

77 www.scirp.org — 8 語 — < 1%
インターネット

78 Jianwei Yue, Ying Chen, Limin Zhao, Siyuan Wang, Huicong Su, Xue Yang, Huijie Gao, Yiang Zhang, Wenhao Li. "Effects of Aging on the Dry Shrinkage Cracking of Lime Soils with Different Proportions", Applied Sciences, 2021 — 7 語 — < 1%
Crossref

79 Mehmet Kurtoğlu, Fatih Eroğlu, Ali Osman Arslan, Ahmet Mete Vural. "Recent contributions and future prospects of the modular multilevel converters: A comprehensive review", International Transactions on Electrical Energy Systems, 2019
Crossref
7 語 — < 1%

80 Control Strategy, Weide Guan, Shoudao Huang, Xiaoqing Huang. "A Medium-Voltage Wind Generation System Based on MPMSG and MMC and Its Fault-Tolerant", 2019 IEEE 3rd International Electrical and Energy Conference (CIEEC), 2019
Crossref
6 語 — < 1%

81 Jung, Jae-Jung, Shenghui Cui, Younggi Lee, and Seung-Ki Sul. "A cell capacitor energy balancing control of MMC-HVDC under the AC grid faults", 2015 9th International Conference on Power Electronics and ECCE Asia (ICPE-ECCE Asia), 2015.
Crossref
6 語 — < 1%

82 Penghan Li, Jie Wang, Linyun Xiong, Meiling Ma, Ziqiang Wang, Sunhua Huang. "Robust sub-synchronous damping controller to mitigate SSCI in series-compensated DFIG-based wind park", IET Generation, Transmission & Distribution, 2020
Crossref
6 語 — < 1%

83 Rosyadi, Marwan, S. M. Muyeen, Rion Takahashi, and Junji Tamura. "A Design Fuzzy Logic Controller for a Permanent Magnet Wind Generator to Enhance the Dynamic Stability of Wind Farms", Applied Sciences, 2012.
Crossref
6 語 — < 1%

84 Shoji Nishikata. "A New Interconnecting Method for Wind Turbine/Generators in a Wind Farm", Green Energy and Technology, 2012
6 語 — < 1%

Crossref

85 Wei Qiao, Ronald G. Harley, Ganesh K. Venayagamoorthy. "Dynamic Modeling of Wind Farms with Fixed-Speed Wind Turbine Generators", 2007 IEEE Power Engineering Society General Meeting, 2007 — 6 語 — < 1%
Crossref

86 Yerraguntla Shasi Kumar, Gautam Poddar. "Balanced Submodule Operation of Modular Multilevel Converter-Based Induction Motor Drive for Wide-Speed Range", IEEE Transactions on Power Electronics, 2020 — 6 語 — < 1%
Crossref

87 opus4.kobv.de — 5 語 — < 1%
インターネット

88 Heinz Schade, Klaus Neemann. "Tensoranalysis", Walter de Gruyter GmbH, 2006 — 4 語 — < 1%
Crossref

引用を除外する	オフ	一致を除外する	オフ
参考文献の除外	オン		